Supplementary Information

for

Morphological regulation of sulfur–vacancy–rich CdS for tunable CO_2 photoreduction under visible irradiation

Lu–Wen Qiu[§], Wen–Ni Zhang[§], Lin–Ying Wang, Hao Li, Tian–Kuan Zhang, Mi–Xin Lin, Su–Qin Ci* and Jian Lü*

Fujian Provincial Key Laboratory of Soil Environmental Health and Regulation, College of Resources and Environment, Fujian Agriculture and Forestry University, No. 15 Shang Xia Dian Road, Fuzhou, 350002, China

[§]Equal contributions.

*Corresponding authors. E–mail: sqci@fafu.edu.cn (S.Q.C.); jian_lu_fafu@fafu.edu.cn (J.L.)

Experimental

Computational Details

The calculations were carried out using density functional theory with the PBE form of generalized gradient approximation functional (GGA).[S1] The Vienna ab−initio simulation package (VASP)[S2−S5] was employed. The plane wave energy cutoff was set as 400 eV. The Fermi scheme was employed for electron occupancy with an energy smearing of 0.1 eV. The first Brillouin zone was sampled in the Monkhorst−Pack grid.[S6] The 3×3×1 k−point mesh for the surface calculation. The energy (converged to 1.0 $\times 10^{-6}$ eV/atom) and force (converged to 0.01 eV/Å) were set as the convergence criterion for geometry optimization.

Model

The model of CdS(002) is built by cutting CdS along the (002) direction according to the experimental observation. Four layers and 3×3 supercell of CdS(002) surface is obtained. To construct the CdS(002) structure with S vacancy, one surface S atom is removed. During the structural optimization calculations, all the atoms were allowed to relax. A vacuum layer as large as 25 Å was used along the c direction normal to the surface to avoid periodic interactions.

Photoelectrochemical measurements

The photoreduction test is carried out at room temperature and pressure filled with CO_2, and a 300W xenon lamp ($\lambda \geq 400$ nm, light intensity = 400 mW/cm^2) is used as the excitation light source. Specifically, 10.0 mg photocatalysts were added to the reactor, which contained 8 mL MeCN and TEA (V = 3:1). Then the reaction system was vacuum degassed and filled with CO_2 and repeated three times to ensure that the reactor was filled with CO_2. In the process of photocatalytic reaction, 1.0 mL gas was taken every 1 h and the product was analyzed by gas chromatography.

Reference

(S1) Perdew, J. P.; Burke, K.; Ernzerhof M. Generalized Gradient Approximation Made Simple. *Phys. Rev. Lett.* **1996**, 77, 3865−3868.

(S2) Kresse, G.; Furthmüller, J. Efficiency of Ab−initio Total Energy Calculations for Metals and Semiconductors Using a Plane−Wave Basis Set. *Comp. Mater. Sci.* **1996**, 6, 15−50.

(S3) Kresse, G.; Hafner, J. Ab initio Molecular Dynamics for Liquid Metals. *Phys. Rev. B* **1993**, 47,

558−561.

(S4) Kresse, G.; Hafner, J. Ab initio Molecular−Dynamics Simulation of the Liquid−Metal–Amorphous−Semiconductor Transition in Germanium. *Phys. Rev. B* 1994, 49, 14251−14269.

(S5) Kresse, G.; Furthmüller, J. Efficient Iterative Schemes for Ab Initio Total−Energy Calculations Using a Plane−Wave Basis Set. *Phys. Rev. B* **1996**, 54, 11169−11186.

(S6) Monkhorst, H. J.; Pack, J. D. Special Points for Brillouin−Zone Integrations. *Phys. Rev. B* **1976**, 13, 5188−5192.

Table S1 A comparison on the CO production rates of CdS based photocatalysts.

Photocatalyst	Sacrificial agent	CO production rate ($\mu mol\ h^{-1}\ g^{-1}$)	Reference
NG/CdS	/	2.6	S7
CdS/TiO2	/	3.6	S8
CdS/FeTCPP	TEOA	7.2	S9
Ni/CdS QDs	TEOA	9.5	S10
ZnS/CdS/rGO	TEOA	9.7	S11
FeOOH/CdS	/	12.6	S12
CdS/Ni(bpy)3Cl2	TEOA	46.9	S13
CdS/Ni9S8/Al2O3	TEOA	121.0	S14
CdS–CuS	TEOA	203.4	S15
w−CdS	TEOA	**372.8**	**This work**
r−CdS	TEOA	**638.7**	**This work**
p–CdS	TEOA	**4058.5**	**This work**

Reference

(S7) Bie, C.; Zhu, B.; Xu. F. et al. In Situ Grown Monolayer N−Doped Graphene on CdS Hollow Spheres with Seamless Contact for Photocatalytic CO_2 Reduction. *Adv. Mater.* **2019**, 31, 1902868.

(S8) Pan, X.; Xu, Y. J. Graphene−Templated Bottom−up Fabrication of Ultralarge Binary CdS–TiO_2 Nanosheets for Photocatalytic Selective Reduction. *J. Phys. Chem. C* **2015**, 119, 7184−7194.

(S9) Li, P.; Hou, C.; Zhang, X. et al. Ethylenediamine−Functionalized CdS/tetra(4−carboxyphenyl)porphyrin Iron(III) Chloride Hybrid System for Enhanced CO_2 Photoreduction. *Appl. Surf. Sci.* **2018**, 459, 292−299.

(S10) Wang, J.; Xia, T.; Wang, L. et al. Enabling Visible−Light−Driven Selective CO_2 Reduction by Doping Quantum Dots: Trapping Electrons and Suppressing H_2 Evolution. *Angew. Chem. Int. Ed.* **2018**, 57, 16447−16451.

(S11) Xu, M.; Jiang, H.; Li, X. et al. Design of A ZnS/CdS/rGO Composite Nanosheet Photocatalyst with Multi−Interface Electron Transfer for High Conversion of CO_2. *Sustain. Energ. Fuels*, **2021**, 5, 4606−4617.

(S12) Li, L.; Guo, C.; Ning, J. et al. Oxygen−Vacancy−Assisted Construction of FeOOH/CdS Heterostructure as An Efficient Bifunctional Photocatalyst for CO_2 Conversion and Water Oxidation. *Appl. Catal. B: Environ.* **2021**, 293, 120203.

(S13) Lin, J.; Qin, B.; Fang, Z. Nickel Bipyridine ($Ni(bpy)_3Cl_2$) Complex Used as Molecular Catalyst for Photocatalytic CO_2 Reduction. *Catal. Lett.* **2019**, 149, 25−33.

(S14) Li, S.; Wang, Q.; Yan, X. et al. Al_2O_3 Support Triggering Highly Efficient Photoreduction of CO2 with H_2O on Noble−Metal−Free $CdS/Ni_9S_8/Al_2O_3$. *Appl. Catal. B: Environ.* **2019**, 240, 174−181.

(S15) Xu. J. Y.; Liu, X. J.; Huang, H. N. et al. Facile Synthesis of Compact CdS−CuS Heterostructures for Optimal CO_2−to−Syngas Photoconversion. *Inorg. Chem. Front.* **2022**, 9, 2150−2160.

Fig. S1. (a) CdS(002) without surface S vacancy; and (b) CdS(002) with surface S vacancy.

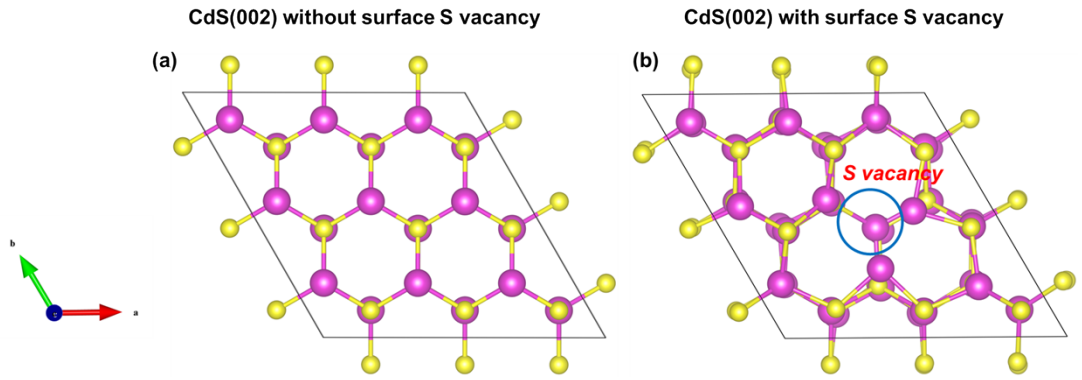

Fig. S2. Optimized structure diagram and charge distribution (sideview).

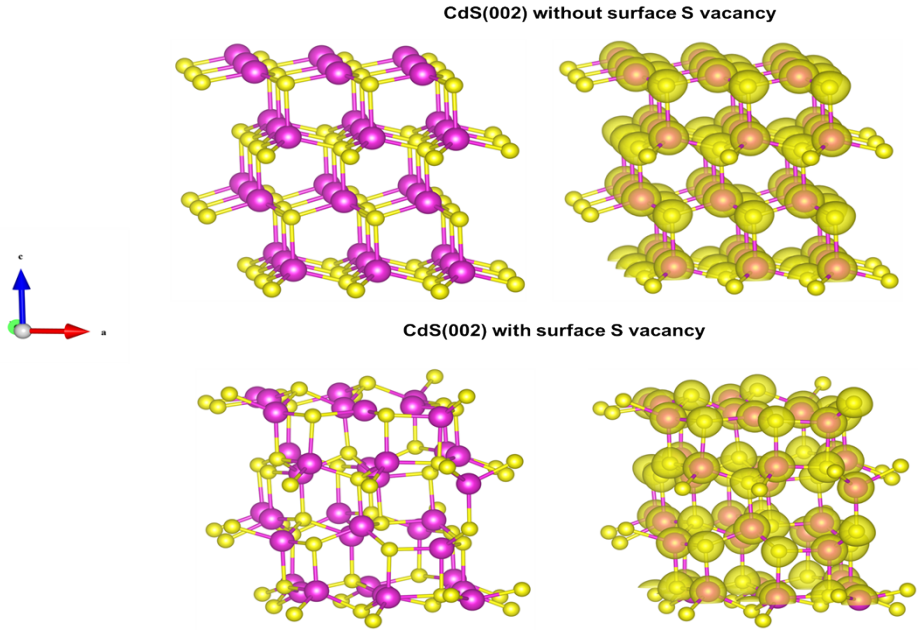

Fig. S3. The charge density maps of the CdS(002) without surface S vacancy (a) and CdS(002) with surface S vacancy (b). (Isosurface=0.1 e/Bohr^3).